Journal Name

Dynamic Article Links ►

Cite this: DOI: 10.1039/c0xx00000x

www.rsc.org/xxxxxx

ARTICLE TYPE

Systematic structural control of multichromic platinum(II)-diimine complexes ranging from ionic solid to coordination polymer

Atsushi Kobayashi,*[a] Hirofumi Hara,[a] Tsubasa Yonemura,[a] Ho-Chol Chang[a] and Masako Kato*[a]

Received (in XXX, XXX) Xth XXXXXXXXX 20XX, Accepted Xth XXXXXXXXX 20XX

DOI: 10.1039/b000000x

Reactions of a Pt(II)-diimine-based metalloligand $Na_2[Pt(CN)_2(4,4'\text{-dcbpy})]$ (4,4'-H_2dcbpy = 4,4'-dicarboxy-2,2'-bipyridine) with alkaline-earth metal salts $Mg(NO_3)_2\cdot 6H_2O$, $CaCl_2$, $SrCl_2\cdot 6H_2O$, and $BaBr_2\cdot 2H_2O$ in aqueous solution gave luminescent complexes formulated as $[Mg(H_2O)_5][Pt(CN)_2(4,4'\text{-dcbpy})]\cdot 4H_2O$ (**MgPt-4·9H$_2$O**), $\{[Ca(H_2O)_3][Pt(CN)_2(4,4'\text{-dcbpy})]\cdot 3H_2O\}_\infty$ (**CaPt-4·6H$_2$O**), $\{[Sr(H_2O)_2][Pt(CN)_2(4,4'\text{-dcbpy})]\cdot H_2O\}_\infty$ (**SrPt-4·3H$_2$O**), and $\{[Ba(H_2O)_2][Pt(CN)_2(4,4'\text{-dcbpy})]\cdot 3H_2O\}_\infty$ (**BaPt-4·5H$_2$O**), respectively. The crystal structures of all **MPt-4** complexes were determined by X-ray crystallography. In these structures, the alkaline-earth metal ions are commonly coordinated to the carboxyl groups of the $[Pt(CN)_2(4,4'\text{-dcbpy})]^{2-}$ metalloligand. In the case of **MgPt-4·9H$_2$O**, the Mg(II) ion is bound by five water molecules and one oxygen atom of a carboxyl group to form a neutral complex molecule $[Mg(H_2O)_5][Pt(CN)_2(4,4'\text{-dcbpy})]$. In contrast, the alkaline-earth metal ion and metalloligand form two-dimensional (**CaPt-4·6H$_2$O**) and three-dimensional (**SrPt-4·3H$_2$O** and **BaPt-4·5H$_2$O**) coordination networks, respectively. All fully hydrated complexes exhibited a strong phosphorescence from the triplet π-π* transition state. Luminescence spectroscopy revealed that **MgPt-4·9H$_2$O** exhibited interesting multichromic (i.e., thermo-, mechano-, and vapochromic) luminescence, whereas **CaPt-4·6H$_2$O** showed only thermochromic luminescence. The other two complexes did not exhibit any chromic behaviour. Combination analysis of powder X-ray diffraction, thermogravimetry, and IR spectroscopy suggests that the dimensionality of the coordination network contributes considerably to both the structural flexibility and luminescence properties; that is, the low-dimensional flexible coordination network formed in **MPt-4** complexes with smaller alkaline-earth metal ions enables a structural rearrangement induced by thermal and mechanical stimuli and vapour adsorption, resulting in the observed multichromic behaviour.

Introduction

One-dimensionally stacked square-planer Pt(II) complexes have attracted considerable attention because of their characteristic coloration, strong luminescence, and interesting chromic behaviours.[1-6] In this system, the metallophilic interaction between the Pt(II) ions is known to play an important role in determining their unique physical properties.[1-2] The overlap between the two $5dz^2$ orbitals of the Pt(II) ions generates an antibonding dσ* orbital near the highest-occupied molecular orbital (HOMO) level. Because the energy of this dσ* orbital strongly depends on the distance between the Pt(II) ions, the colour and/or luminescence of the solid can be widely tuned by manipulating the Pt(II)-Pt(II) distance.[3-4] In 1995, Mann *et al.* reported that intermolecular metallophilic interactions between d^8 metal ions play a critical role in the vapochromic behaviour of these complexes.[5] By exploiting these distance-dependent chromophoric properties, researchers have synthesized many vapochromic Pt(II) complexes.[5-6] For example, Chen *et al.* reported the unique vapochromic behaviour of a neutral Pt(II) complex $[Pt(Me_3SiC{\equiv}CbpyC{\equiv}CSiMe_3)(PhC{\equiv}C)_2]$ that varied the colour depending on the molecular weight of the hydrocarbons.[6o] In addition, some Pt(II) and Au(I) complexes have been recently found to exhibit interesting mechanochromic behaviour.[7] However, to the best of our knowledge, there are still few complexes that show the double-, triple-, and multichromic behaviours present in this Pt(II)-diimine series.[7d]

We recently reported a chromic coordination polymer (CCP), $\{[Zn(H_2O)_3][Pt(CN)_2(5,5'\text{-dcbpy})]\cdot H_2O\}_n$ (**ZnPt-5**·4H$_2$O), built from a Zn(II) ion and a Pt(II)-diimine-based metalloligand $[Pt(CN)_2(5,5'\text{-}H_2\text{dcbpy})]$ (5,5'-H_2dcbpy = 5,5'-dicarboxy-2,2'-bipyridine),[8] because the structure of coordination polymer (CP) can be easily and widely modified by replacement of metal ions and bridging ligands.[9-11] We found that the metallophilic interaction between the Pt(II) atoms results in the metalloligands acting as chromic centres even within a relatively rigid coordination network, resulting in thermochromic and *insoluble* solvatochromic behaviours. In addition, the replacement of bridging metal ion from Zn^{2+} to alkaline-earth metal ions significantly affected both the vapour-adsorption property and solid-state solvatochromic behaviour.[8b] However, the one-

dimensional coordination-network structure built from the alternate arrangement of M^{2+} ion and the metalloligand $[Pt(CN)_2(5,5'\text{-dcbpy})]^{2-}$ is commonly formed, resulting in the limitation of the structural control of the coordination-network structure. Thus, in this work, to control both the chromotoropic behavior and coordination-network structure constructed by the Pt(II)-diimine-based metalloligand, we have synthesized four Pt(II)-diimine-based complexes using the isomeric metalloligand, $[Pt(CN)_2(4,4'\text{-dcbpy})]^{2-}$ with alkaline-earth metal ions, namely, $[Mg(H_2O)_5][Pt(CN)_2(4,4'\text{-dcbpy})]\cdot 4H_2O$ (**MgPt-4·9H$_2$O**), $\{[Ca(H_2O)_3][Pt(CN)_2(4,4'\text{-dcbpy})]\cdot 3H_2O\}_n$ (**CaPt-4·6H$_2$O**), $\{[Sr(H_2O)_2][Pt(CN)_2(4,4'\text{-dcbpy})]\cdot H_2O\}_n$ (**SrPt-4·3H$_2$O**), and $\{[Ba(H_2O)_2][Pt(CN)_2(4,4'\text{-dcbpy})]\cdot 3H_2O\}_n$ (**BaPt-4·5H$_2$O**). We found the position of the carboxyl group on the dcbpy ligand significantly affected not only the crystal structures but also the luminescence properties and chromic behaviours, that is, the **MgPt-4·9H$_2$O** complex, without any infinite coordination network, showed interesting multichromic (thermo-, vapo-, and mechanochromic) luminescence, whereas **CaPt-4·6H$_2$O**, with a two-dimensional coordination-sheet structure, showed only thermochromic luminescence. The other two coordination polymers (CPs), which featured three-dimensional coordination networks, did not show any chromic behaviour. Although there are many chromic materials that use the Pt(II)-diimine complexes as chromophores,[5-6] **MgPt-4·9H$_2$O** is a very rare example of a material that exhibits triple chromic behaviour. In this paper, we discuss the syntheses, crystal structures, and chromic behaviours of these Pt(II)-diimine-based **MPt-4·*n*H$_2$O** complexes on the basis of X-ray structural determinations, powder X-ray diffraction measurements, and luminescence and IR spectroscopy.

Experimental Section

Syntheses

All starting materials, K_2PtCl_4, $Mg(NO_3)_2\cdot 6H_2O$, $CaCl_2$, $SrCl_2\cdot 6H_2O$, $BaBr_2\cdot 2H_2O$, and 3-methylpyridine were used as received from commercial sources, and the solvents were used without any purification. Unless otherwise stated, all manipulations were performed in air. $Na_2[Pt(CN)_2(4,4'\text{-dcbpy})]\cdot 2H_2O$ was prepared according to a published method.[6p] Elemental analysis was performed at the analysis centre in Hokkaido University.

Synthesis of $[Mg(H_2O)_5][Pt(CN)_2(4,4'\text{-dcbpy})]\cdot 4H_2O$ (MgPt-4·9H$_2$O): $Na_2[Pt(CN)_2(4,4'\text{-dcbpy})]\cdot 2H_2O$ (10 mg, 17 μmol) was dissolved in water (0.5 ml). To this clear pale-yellow solution, an aqueous solution (0.5 ml) of $Mg(NO_3)_2\cdot 6H_2O$ (5.3 mg, 20 μmol) was added, resulting in the gradual emergence of an orange precipitate. After standing at room temperature for 3 days, the orange precipitate changed to pale-yellow platelet crystals. The crystals were collected by filtration and washed with a small amount of water and then dried in air for 1 day to afford **MgPt-4·9H$_2$O** (6.9 mg) in a 59% yield. One of the single crystals was used for X-ray structural determination. Elemental analysis for $C_{14}H_6N_4O_4PtMg\cdot 9H_2O$; calcd.: C 24.88, H 3.58, N 8.29; found: C 24.41, H 3.39, N 8.35. IR (KBr, cm^{-1}): 3391 s, 2159 s, 2148 s, 1606 s, 1552 s, 1434 w, 1411 w, 1382 s, 1302 w, 1277 w, 1245 m, 1159 w, 1108 w, 1072 m, 1038 w, 920 w, 877 w, 788 m, 708 m, 475 w.

Synthesis of $\{[Ca(H_2O)_3][Pt(CN)_2(4,4'\text{-dcbpy})]\cdot 3H_2O\}_n$ (CaPt-4·6H$_2$O): $Na_2[Pt(CN)_2(4,4'\text{-dcbpy})]\cdot 2H_2O$ (10 mg, 17 μmol) was dissolved in water (0.5 ml). To this clear pale-yellow solution, an aqueous solution (0.5 ml) of $CaCl_2$ (2.4 mg, 21 μmol) was added resulting in the gradual emergence of an orange precipitate. After standing at room temperature for 2 weeks, the orange precipitate changed slowly to pale-yellow needle-like crystals. The crystals were collected by filtration and washed with a small amount of water and then dried in air for 1 day to afford **CaPt-4·6H$_2$O** (4.2 mg) in a 39% yield. One of the single crystals was used for X-ray structural determination. Elemental analysis for $C_{14}H_6N_4O_4PtCa\cdot 6H_2O$; calcd.: C 26.38, H 2.85, N 8.79; found: C 26.10, H 2.88, N 8.47. IR (KBr, cm^{-1}): 3404 s, 3074 w, 2160 s, 2143 s, 1603 s, 1550 s, 1445 m, 1418 s, 1392 s, 1291 w, 1244 m, 1164 w, 1115 w, 1070 w, 1040 w, 924 w, 872 w, 798 w, 787 m, 716 m, 475 w.

Synthesis of $\{[Sr(H_2O)_2][Pt(CN)_2(4,4'\text{-dcbpy})]\cdot H_2O\}_n$ (SrPt-4·3H$_2$O): $Na_2[Pt(CN)_2(4,4'\text{-dcbpy})]\cdot 2H_2O$ (20 mg, 35 μmol) was dissolved in water (2 ml). To this clear pale-yellow solution, an aqueous solution (1 ml) of $SrCl_2\cdot 6H_2O$ (9.5 mg, 35.6 μmol) was added resulting in the rapid precipitation of a pale-yellow solid. After stirring for 1 h at room temperature, the precipitate was collected by filtration and washed with a small amount of water and then dried in air for 1 day to afford **SrPt-4·3H$_2$O** (19 mg) in an 86% yield. Pale-yellow single crystals suitable for X-ray crystallographic analysis were obtained by the diffusion of a $SrCl_2$ ethanol solution into an aqueous solution of $Na_2[Pt(CN)_2(4,4'\text{-dcbpy})]\cdot 2H_2O$. Elemental analysis for $C_{14}H_6N_4O_4PtSr\cdot 3H_2O$; calcd.: C 26.65, H 1.92, N 8.88; found: C 26.71, H 1.78, N 8.74. IR (KBr, cm^{-1}): 3433 s, 3080 w, 2165 s, 2145 s, 1620 s, 1589 s, 1551 s, 1448 m, 1413 s, 1384 s, 1307 w, 1284 w, 1244 m, 1169 w, 1109 w, 1069 w, 1039 w, 918 w, 864 m, 810 w, 798 w, 785 m, 774 w, 713 m, 476 w.

Synthesis of $\{[Ba(H_2O)_2][Pt(CN)_2(4,4'\text{-dcbpy})]\cdot 3H_2O\}_n$ (BaPt-4·5H$_2$O): $Na_2[Pt(CN)_2(4,4'\text{-dcbpy})]\cdot 2H_2O$ (20 mg, 35 μmol) was dissolved in water (2 ml). To this clear pale-yellow solution, an aqueous solution (1 ml) of $BaBr_2\cdot 2H_2O$ (12 mg, 36 μmol) was added resulting in the rapid precipitation of a pale-yellow solid. After subsequent stirring for 1 h at room temperature, the precipitate was collected by filtration and washed with a small amount of water and then dried in air for 1 day to afford **BaPt-4·5H$_2$O** (21 mg) in an 84% yield. Pale-yellow single crystals suitable for X-ray crystallographic analysis were obtained by the diffusion of a $BaBr_2$ ethanol solution into an aqueous solution of $Na_2[Pt(CN)_2(4,4'\text{-dcbpy})]\cdot 2H_2O$. Elemental analysis for $C_{14}H_6N_4O_4PtBa\cdot 5H_2O$; calcd.: C 23.46, H 2.25, N 7.82; found: C 23.18, H 2.19, N 7.63. IR (KBr, cm^{-1}): 3422 s, 3078 w, 2157 s, 2146 s, 1617 s, 1583 s, 1550 s, 1438 w(sh), 1411 w(sh), 1384 s, 1287 w, 1243 m, 1106 w, 1071 w, 1038 w, 918 w, 861 w, 785 m, 709 m, 478 w.

Single-crystal X-ray structural determination.

All single-crystal X-ray diffraction measurements were performed using a Rigaku Mercury CCD diffractometer with graphite monochromated Mo Kα radiation (λ= 0.71069 Å) and a rotating anode generator. Each single crystal was mounted on a MicroMount with paraffin oil. A nitrogen gas flow temperature controller was used to cool the sample. Diffraction data were collected and processed using CrystalClear.[12] The structure was solved by a direct method using SIR2004,[13] and refined by full-matrix least squares using SHELXL-97.[14] The non-hydrogen atoms in **MgPt-4·9H$_2$O**, **CaPt-4·6H$_2$O** and **BaPt-4·5H$_2$O** were refined anisotropically. In the case of **SrPt-4·3H$_2$O**, the carbon and nitrogen atoms of the bipyridine rings were refined isotropically and the other non-hydrogen atoms were refined anisotropically due to the poor crystallinity. Disordered water molecules in **CaPt-4·6H$_2$O** were taken into account using PLATON/SQUEEZE.[15] Hydrogen atoms were refined using the

riding model. All calculations were performed using the Crystal Structure crystallographic software package.[16] The obtained crystallographic data for each complex are summarized in Table 1.

Table 1 Crystal parameters and refinement data.

Complex	**MgPt-4·9H$_2$O**	**CaPt-4·6H$_2$O**	**SrPt-4·3H$_2$O**	**BaPt-4·5H$_2$O**
T / K	173(1)	150(1)	150(1)	150(1)
Formula	$C_{14}H_6N_4O_4Pt$ Mg·9H$_2$O	$C_{14}H_6N_4O_4Pt$ Ca·6H$_2$O	$C_{14}H_6N_4O_4Pt$ Sr·3H$_2$O	$C_{14}H_6BaN_4O_4$ Pt·5H$_2$O
Formula weight	675.76	637.49	630.98	716.72
Crystal system	Triclinic	Monoclinic	Triclinic	Monoclinic
Space group	P-1	$P2_1/n$	P-1	$P2_1/n$
a / Å	6.924(4)	7.1293(19)	7.072(2)	7.3068(19)
b / Å	13.689(8)	17.848(4)	10.385(4)	17.634(5)
c / Å	13.933(7)	16.168(4)	12.842(4)	15.226(4)
α / °	114.208(5)	90	100.695(6)	90
β / °	95.815(4)	96.7810(14)	91.181(6)	94.4477(11)
γ / °	104.400(4)	90	94.614(6)	90
V / Å^3	1135.4(10)	2043.0(9)	923.2(5)	1955.9(9)
Z	2	4	2	4
$D_{cal.}$/ g·cm^{-3}	1.977	2.080	2.270	2.434
Reflections collected	9040	16257	7348	15324
Unique reflections	5085	4675	4062	4476
GOF	1.104	1.004	0.965	1.061
R_{int}	0.040	0.070	0.047	0.052
R (I > 2.00σ(I))	0.0518	0.0335	0.0693	0.0393
R_W [a]	0.1549	0.0826	0.1907	0.0839

[a] $R_W = [\Sigma(w (F_o^2 - F_c^2)^2)/\Sigma w(F_o^2)^2]^{1/2}$

Powder X-ray diffraction.

Powder X-ray diffraction (PXRD) measurements at various temperatures were performed using a Rigaku SPD diffractometer at beamline BL-8B at the Photon Factory, KEK, Japan. The wavelength of the synchrotron X-ray was 1.200(1) Å. The sample was placed in a glass capillary with a 0.5-mm diameter. The temperature of the sample was controlled using a nitrogen gas flow variable temperature controller.

Luminescence spectroscopy.

Luminescence spectra were recorded under various conditions on a Jasco FP-6600 spectrofluorometer. The sample temperature was controlled by a JASCO ETC-273 Peltier-type temperature controller. About 1 mg of the sample was placed in a glass capillary with a 0.5-mm diameter. The slit widths of the excitation and emission light were 5 and 6 nm, respectively.

Luminescence quantum efficiency measurements.

The luminescence quantum efficiency of each sample in the solid state was recorded using a Hamamatsu C9920-02 absolute photoluminescence quantum yield measurement system equipped with an integrating sphere apparatus and a 150 W CW Xenon light source.

Luminescence lifetimes.

The luminescence lifetime of each sample was recorded using a Hamamatsu C4780 Picosecond Fluorescence Lifetime Measurement System equipped with a nitrogen laser light source (λ = 337.1 nm).

Thermogravimetric analysis.

Thermogravimetry and differential thermal analysis were performed using a Rigaku ThermoEvo TG8120 analyzer.

IR spectroscopy.

The IR spectrum of each complex was recorded on a Nicolet 6700 FT-IR spectrometer equipped with a Smart-Orbit (Diamond) ATR accessory.

Results and discussion

Crystal structures.

Figure 1(a) shows the molecular structure of **MgPt-4·9H$_2$O**. The complex crystallized in the triclinic P-1 space group. The Mg(II) ion is surrounded by one carboxyl oxygen of the $[Pt(CN)_2(4,4'\text{-dcbpy})]^{2-}$ metalloligand and five water molecules to form a neutral molecule, $\{[Mg(H_2O)_5][Pt(CN)_2(4,4'\text{-dcbpy})]\}$. The average Mg-O(water) bond distances ranged from 2.06–2.09 Å, which is consistent with the oxygen atoms originating from water molecules as opposed to anionic hydroxide ions. In the $[Pt(CN)_2(4,4'\text{-dcbpy})]^{2-}$ moiety, all atoms except for the carboxyl oxygens lie on the PtC_2N_2 coordination plane. The bond lengths and angles around the metalloligand are very similar to those in the sodium salt, $Na_2[Pt(CN)_2(4,4'\text{-dcbpy})]\cdot 5H_2O$ (see Table S1 in supporting information). In the case of the protonated complex $[Pt(CN)_2(4,4'\text{-}H_2\text{dcbpy})]$, the Pt(II) ions formed a one-

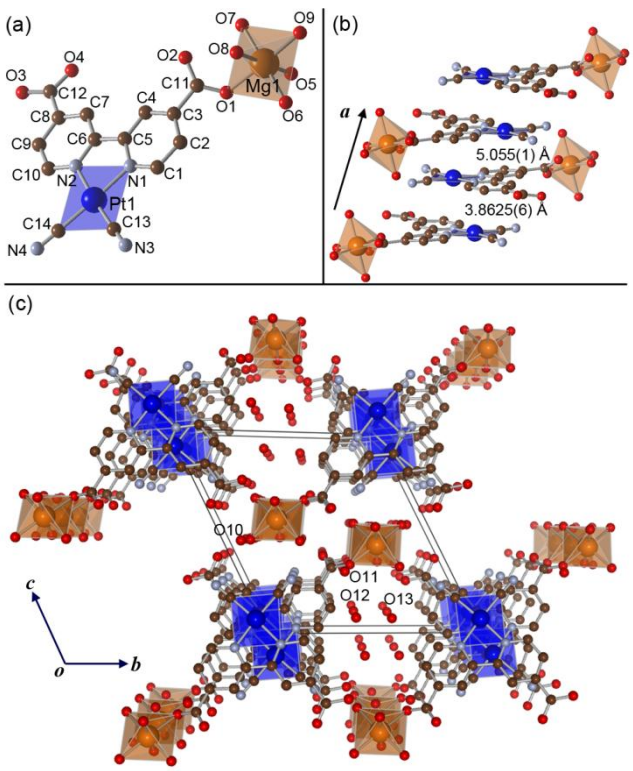

Fig. 1 (a) Molecular structure, (b) 1-D stacked structure, and (c) packing diagram viewed down along the a axis of **MgPt-4·9H$_2$O**. The coordination spheres of the Pt(II) and Mg(II) ions are shown as blue planes and orange octahedrons, respectively. H atoms are omitted for clarity. Solvated water molecules are omitted in (a) and (b) for clarity. The brown, light-blue, and red spheres represent C, N, and O atoms, respectively.[18]

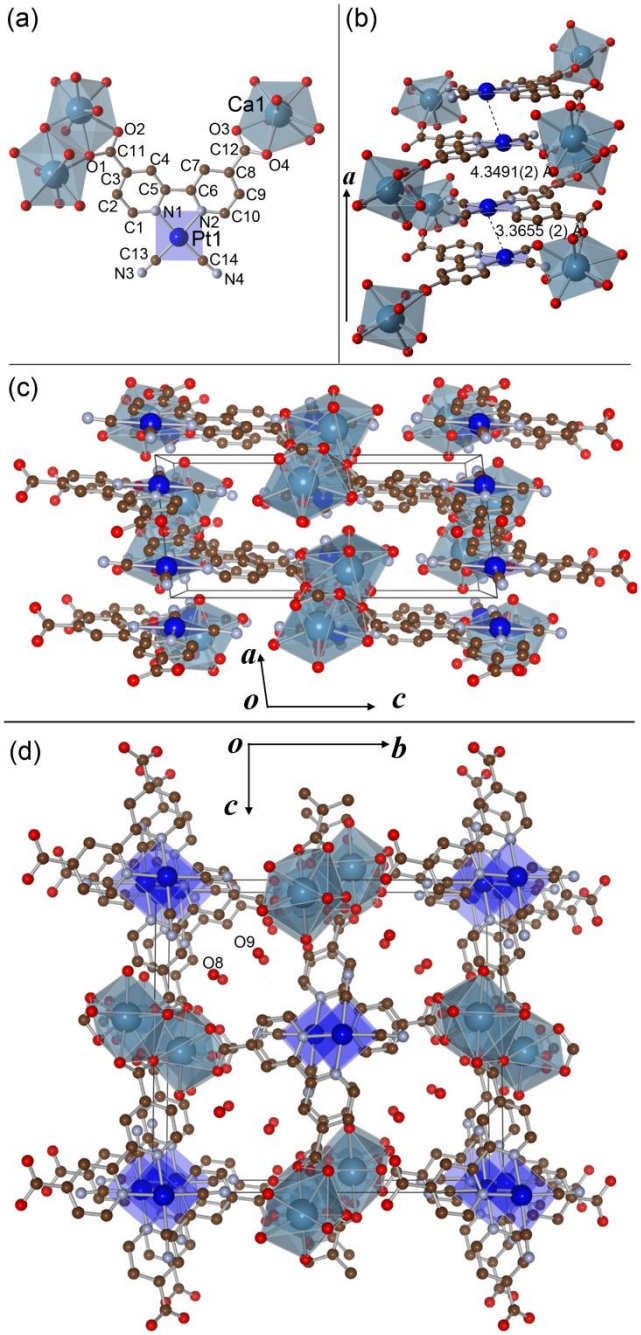

Fig. 2 (a) Asymmetric unit, (b) 1-D stacked structure, and (c) packing diagrams viewed down along the *b* and (d) *a* axes of **CaPt-4·6H$_2$O**. The coordination spheres of the Pt(II) and Ca(II) ions are shown as blue planes and grayish blue polyhedrons, respectively. The dotted lines represent the effective metallophilic interaction between Pt(II) ions. H atoms are omitted for clarity. Solvated water molecules are omitted in (a), (b), and (c) for clarity. Brown, light-blue, and red spheres represent C, N, and O atoms, respectively.[18]

dimensional (1-D) column with effective metallophilic interaction at a distance of 3.3 Å.[6h] In contrast, the Pt(II) ions in **MgPt-4·9H$_2$O** form a zigzag-type chain structure, as shown in Figure 1(b), and even the shortest distance between neighboring Pt(II) ions is over 3.7 Å. This result indicates that the metallophilic interaction between the Pt(II) ions in **MgPt-4·9H$_2$O** is negligibly weak. It should be noted that there are nine water molecules in

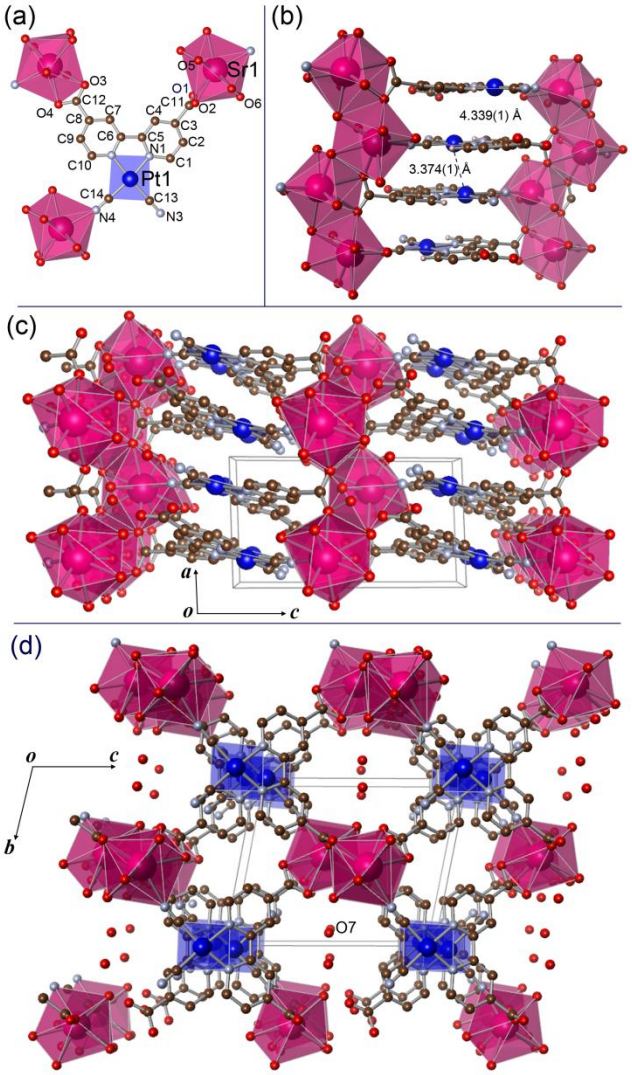

Fig. 3 (a) Asymmetric unit, (b) 1-D stacked structure, and (c) packing diagrams viewed down along the *b* and (d) *a* axes of **SrPt-4·3H$_2$O**. The coordination spheres of the Pt(II) and Sr(II) ions are shown as blue planes and purple polyhedrons, respectively. The dotted lines represent the effective metallophilic interaction between Pt(II) ions. H atoms are omitted for clarity. Solvated water molecules are omitted in (a), (b), and (c) for clarity. Brown, light-blue, and red spheres represent C, N, and O atoms, respectively.[18]

one unit cell, i.e., five coordinated to the Mg(II) ion and four crystal water molecules. Two of the four crystal water molecules (O10 and O11) are tightly bound by four hydrogen bonds. In contrast, the other two water molecules (O12 and O13) form only one hydrogen bond to the tightly bound crystal water, resulting in larger temperature factors. The latter water molecules form a water channel along the *a* axis, as shown in Figure 1(c).

Figure 2(a) shows the structure of **CaPt-4·6H$_2$O** in one asymmetric unit. The complex **CaPt-4·6H$_2$O** crystallized in the monoclinic $P2_1/n$ space group. Only one crystallographically independent Ca(II) ion and the $[Pt(CN)_2(4,4'\text{-dcbpy})]^{2-}$ metalloligand were found in the unit cell. The Ca(II) ion is surrounded by five carboxyl oxygen atoms and three water molecules, resulting in an eight-coordinate structure. The metalloligand $[Pt(CN)_2(4,4'\text{-dcbpy})]^{2-}$ is bound to three Ca(II) ions, as shown in Figure 2(a). The oxygen atoms from one of the

two carboxyl groups (O3 and O4) are bound to a Ca ion in a bidentate fashion. The oxygen atoms of another carboxyl group (O1 and O2) are also coordinated to the Ca ion in a bidentate fashion, but the O1 atom also bridges to the adjacent Ca ion (Figure 2(a)). The $[Pt(CN)_2(4,4'\text{-dcbpy})]^{2-}$ units stack with a zigzag-type chain arrangement along the *a* axis, as shown in Figure 2(b). Owing to an effective metallophilic interaction between the Pt(II) ions, the $[Pt(CN)_2(4,4'\text{-dcbpy})]^{2-}$ units are moderately dimerized, with the shortest adjacent Pt-Pt distance being 3.3655(2) Å (Figure 2(b)). As a result of the crosslink of the Ca ions by the metalloligands, an infinite two-dimensional coordination-bonded sheet is formed on the (101) plane, as shown in Figure 2(c). Three coordinated water molecules and two crystal water molecules were found in one unit cell. These crystal water molecules form 1-D water channels along the *a* axis, as shown in Figure 2(d).

Figure 3(a) shows the structure of **SrPt-4·3H$_2$O** in one asymmetric unit. The complex **SrPt-4·3H$_2$O** crystallized in the triclinic *P*-1 space group. Similar to **CaPt-4·6H$_2$O**, only one crystallographically independent Sr(II) ion and $[Pt(CN)_2(4,4'\text{-dcbpy})]^{2-}$ were found in the unit cell. The Sr(II) ion is coordinated by five carboxyl oxygens, two water molecules, and one cyano nitrogen, resulting in a eight-coordinate structure. The metalloligand $[Pt(CN)_2(4,4'\text{-dcbpy})]^{2-}$ is bound to five Sr(II) ions. The oxygen atoms from one of the two carboxyl groups (O3 and O4) are bound to the Sr ion in a simple bidentate fashion. Although the oxygen atoms of another carboxyl group (O1 and O2) are also coordinated to the Sr ion in a bidentate mode, these oxygen atoms also bridge to the adjacent Sr ions (Figure 3(b)), resulting in the formation of a 1-D coordination chain along the *a* axis. In contrast to **MgPt-4·9H$_2$O** and **CaPt-4·6H$_2$O**, one of the two cyano ligands is bonded to the Sr ion. However, similar to **CaPt-4·6H$_2$O**, the $[Pt(CN)_2(4,4'\text{-dcbpy})]^{2-}$ units stack to form zigzag-type 1-D columns along the *a* axis, as shown in Figure 3(b). In this column, the shortest distance between Pt(II) ions is 3.374(1) Å, which is slightly longer than that in **CaPt-4·6H$_2$O** (3.3655(2) Å), suggesting that the metallophilic interaction is slightly weaker in **SrPt-4·3H$_2$O**. There are no effective π-π interactions between adjacent dcbpy ligands in **SrPt-4·3H$_2$O** in this column. Owing to both the larger coordination and lower hydration numbers of the Sr(II) ion, this complex has the three-dimensional coordination-bonded rigid structure shown in Figures 3(c) and (d). One of the three water molecules are not directly coordinated to any Sr(II) ions, but are instead hydrogen-bonded to the carboxyl oxygen or cyano nitrogen atoms. In this complex, 1-D water channels are also formed along the *a* axis.

Figure 4(a) shows the structure of **BaPt-4·5H$_2$O** in one asymmetric unit. The complex **BaPt-4·5H$_2$O** crystallized in the monoclinic $P2_1/n$ space group, and the crystal structure is very similar to that of **SrPt-4·3H$_2$O**. Similar to **CaPt-4·6H$_2$O and SrPt-4·3H$_2$O**, only one crystallographically independent Ba(II) ion and $[Pt(CN)_2(4,4'\text{-dcbpy})]^{2-}$ were found in the unit cell. The Ba(II) ion is surrounded by six carboxyl oxygens, two water molecules, and one cyano nitrogen, resulting in a nine-coordinate structure. The metalloligand $[Pt(CN)_2(4,4'\text{-dcbpy})]^{2-}$ is bound to five Ba(II) ions, as shown in Figure 4(a). The oxygen atoms from one of the two carboxyl groups (O3 and O4) are bound to the Ba ion in a bidentate fashion. Although the oxygen atoms of another

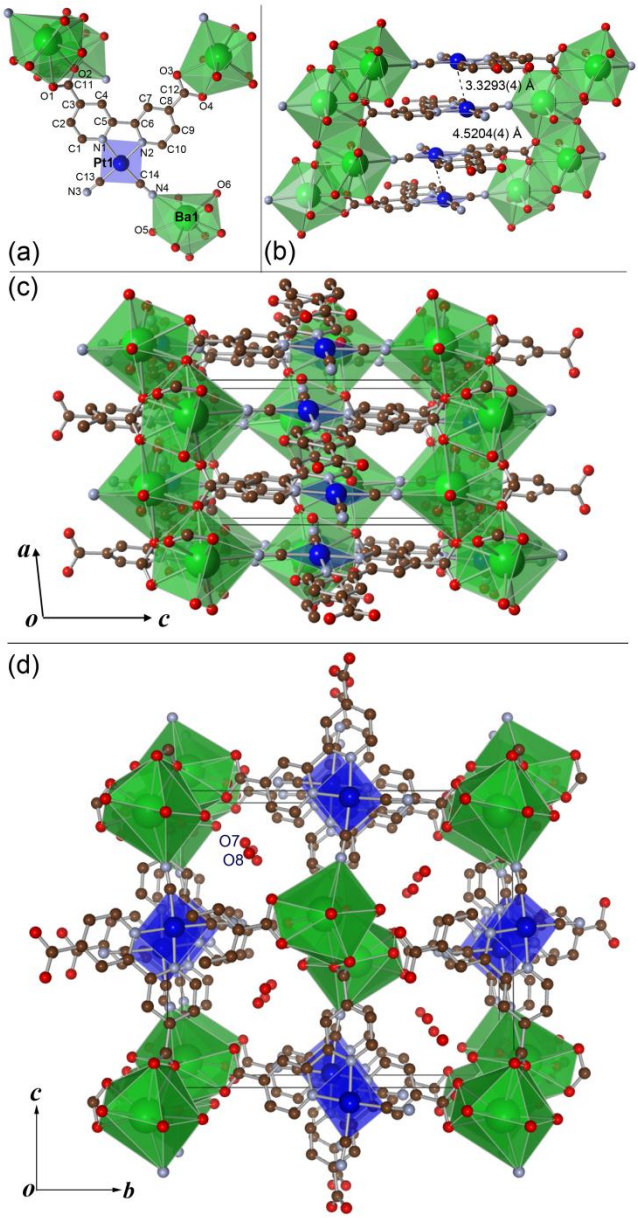

Fig. 4 (a) Asymmetric unit, (b) 1-D stacked structure, and (c) packing diagrams viewed down along the *b* and (d) *a* axes of **BaPt-4·5H$_2$O**. The coordination spheres of the Pt(II) and Ba(II) ions are shown as blue planes and green polyhedrons, respectively. The dotted lines represent the effective metallophilic interaction between Pt(II) ions. H atoms are omitted for clarity. Solvated water molecules are omitted in (a), (b), and (c) for clarity. Brown, light-blue, and red spheres represent C, N, and O atoms, respectively.[18]

carboxyl group (O1 and O2) are also coordinated to the Ba ion in a bidentate mode, these oxygen atoms also bridge to the adjacent Ba ions (Figure 4(a)), resulting in the formation of a 1-D coordination chain along the *a* axis. Similar to **SrPt-4·3H$_2$O**, one of the two cyano ligands is bonded to the Ba(II) ion. The $[Pt(CN)_2(4,4'\text{-dcbpy})]^{2-}$ units stack to form zigzag-type 1-D columns along the *a* axis, as shown in Figure 4(b). In this column, the shortest distance between Pt(II) ions is 3.3293(4) Å, which is slightly shorter than that in **CaPt-4·6H$_2$O** (3.3655(2) Å), suggesting that the metallophilic interaction is more pronounced in **BaPt-4·5H$_2$O**. There are no effective π-π interactions between

adjacent dcbpy ligands in **BaPt-4·5H$_2$O** in this column. Owing to both the larger coordination and lower hydration numbers of the Ba(II) ion, this complex has the three-dimensional coordination-bonded rigid structure shown in Figures 4(c) and (d). Three of the five water molecules are not directly coordinated to any Ba(II) ions, but are instead hydrogen-bonded to the carboxyl oxygen or cyano nitrogen atoms. In this complex, 1-D water channels are also formed along the *a* axis.

As discussed above, the heavier and larger alkaline-earth metal ions tend to form higher-dimensional coordination-network structures. This trend is probably due to the larger ionic radius of the metal ions and the smaller hydration enthalpy. As the ionic radius of an ion grows larger, the ion adopts a larger coordination number. In addition, an ion with a smaller absolute value of hydration enthalpy would tend to form an ionic bond with the anionic ligand-like carboxylate rather than a neutral water molecule. Consequently, the variation of the alkaline-earth metal ion in this **MPt-4·*n*H$_2$O** series enables us to modify not only the hydration number but also the rigidity and dimensionality of the coordination-network structure.

Thermochromic luminescence.

Figure 5 shows the temperature dependence of the luminescence spectra of the four complexes, **MgPt-4·9H$_2$O**, **CaPt-4·6H$_2$O**, **SrPt-4·3H$_2$O**, and **BaPt-4·5H$_2$O**, at room temperature and 373 K. The photophysical properties of these complexes are summarized in Table 2. The synthesized pale-yellow crystals of **MgPt-4·9H$_2$O** and **CaPt-4·6H$_2$O** showed greenish yellow luminescence. The spectrum with vibronic structures with a

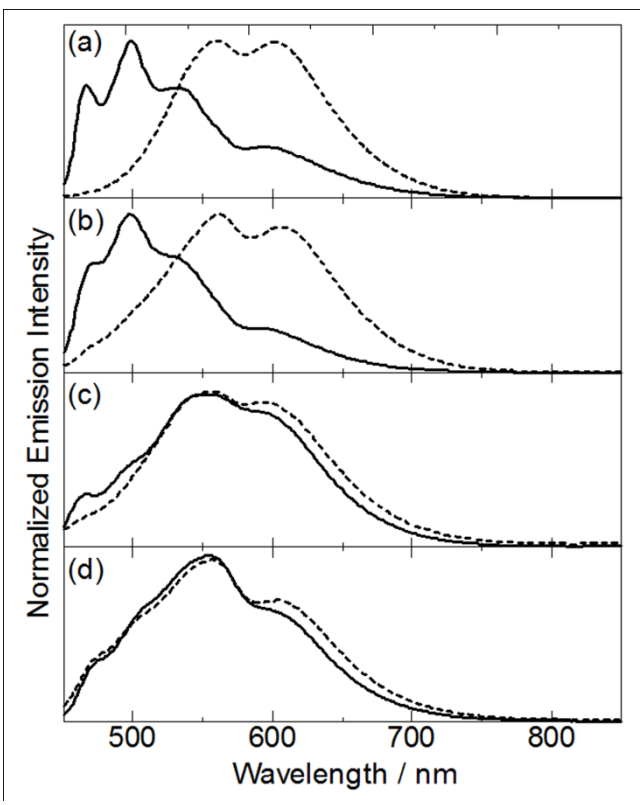

Fig. 5 Temperature dependences of luminescence spectra of (a) **MgPt-4·9H$_2$O**, (b) **CaPt-4·6H$_2$O**, (c) **SrPt-4·3H$_2$O**, and (d) **BaPt-4·5H$_2$O** ($\lambda_{ex.}$ = 400 nm). The solid and broken lines represent the spectra at room temperature and 373 K, respectively.

Table 2 Photophysical properties of **MPt-4·*n*H$_2$O** complexes.

Complex	$\lambda_{em.}$ (RT) / nm [a]	$\lambda_{em.}$ (100 °C) / nm [a]	$\tau_{em.}$ (RT) / μs [b]	$\Phi_{em.}$ (RT) [a]
MgPt-4·9H$_2$O	498	560	3.25	0.21
CaPt-4·6H$_2$O	498	562	1.47	0.27
SrPt-4·3H$_2$O	557	555	0.27	0.09
BaPt-4·5H$_2$O	555	557	0.48	0.11

[a] $\lambda_{ex.}$ = 400 nm [b] $\lambda_{ex.}$ = 337.1 nm.

maximum at 498 nm is assignable to the emission from the $^3\pi$–π^* state, which is mainly localized on the dcbpy ligand. Although the emission maxima of the other two complexes were observed at 556 nm, the vibronic structures are almost the same as those of **MgPt-4·6H$_2$O** and **CaPt-4·6H$_2$O**, implying that they originate from the same $^3\pi$–π^* emission. The observed relatively long emission lifetimes, which ranged from 0.27 to 3.25 μs for the **MPt-4** complexes, are also consistent with this assignment. As discussed earlier, the shortest intermolecular distances between Pt(II) ions in these complexes suggest that metallophilic interactions are not present in **MgPt-4·9H$_2$O**, but are effective in **CaPt-4·6H$_2$O** and **BaPt-4·5H$_2$O**, which feature shortest intermolecular Pt···Pt distances of 3.3655(2) and 3.3293(4) Å, respectively. It is well known that one-dimensionally stacked Pt(II) complexes with effective metallophilic interactions usually exhibit strong phosphorescence from the triplet metal-metal-to-ligand charge-transfer (^{3}MMLCT) state.[3-4] Nevertheless, the origin of the emission for each **MPt-4** is the $^3\pi$–π^* state, implying that the metallophilic interactions in **CaPt-4·6H$_2$O** and **BaPt-4·5H$_2$O** are not strong enough to change the emission origin from the $^3\pi$–π^* to the ^{3}MMLCT state. In fact, the relatively long emission lifetimes of about 1 μs and their characteristic vibronic structures in the emission spectra are quite comparable to the emission from the $^3\pi$-π^*(bpy) state observed for[Pt(CN)$_2$(dC$_9$bpy)] (dC$_9$bpy = 4,4'-dinonyl-2,2'-bipyridine) in a CHCl$_3$ solution.[2i] It is noteworthy that after heating to 373 K, the luminescence spectra of **MgPt-4·9H$_2$O** and **CaPt-4·6H$_2$O** changed to spectra similar to those of the other two **MPt-4** (M = Sr^{2+} and Ba^{2+}) featuring two main emission bands at 560 and 602 nm. The emission lifetime of **MgPt-4·9H$_2$O** after heating at 373 K was about 0.3 μs, which is about one-tenth of the lifetime of the room-temperature **MgPt-4·9H$_2$O** and comparable to that of **SrPt-4·3H$_2$O** (see Table 2). In contrast, **SrPt-4·3H$_2$O** and **BaPt-4·5H$_2$O** showed almost temperature-independent luminescence. In both cases, the similar vibronic structures observed in the spectra suggest that the emission origin, i.e., the $^3\pi$–π^* state, remains unchanged.

In order to account for the mechanisms of the thermochromic luminescence, thermogravimetric (TG) analysis and powder X-ray diffraction (PXRD) measurement were performed. TG analyses of the four **MPt-4·*n*H$_2$O** complexes revealed that heating at 373 K removed almost all of the water molecules to form anhydrous **MPt-4** (see Figure S1). Figure 6 shows the changes in the PXRD patterns of **MgPt-4·9H$_2$O** and **CaPt-4·6H$_2$O**. The PXRD patterns observed for anhydrous **MgPt-4** and **CaPt-4** after drying **MgPt-4·9H$_2$O** and **CaPt-4·6H$_2$O** at 373 K for 1 day were completely different to those of the original hydrates. In contrast, the PXRD pattern of **BaPt-4·5H$_2$O** was not changed after increasing the temperature (see Figure S2). Thus, the thermochromic luminescences of both complexes are

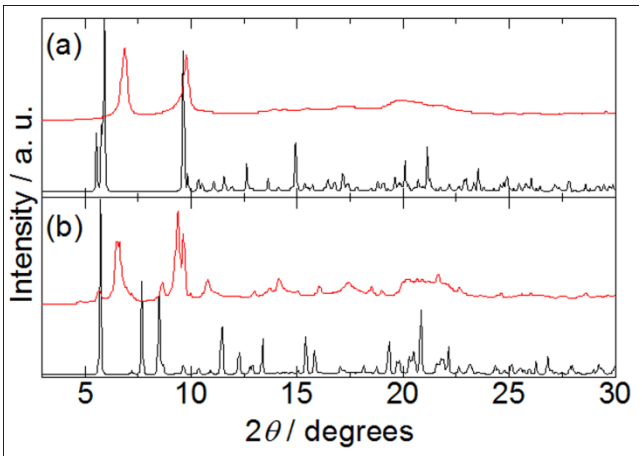

Fig. 6 Temperature dependence of PXRD patterns of (a) **MgPt-4·9H$_2$O** and (b) **CaPt-4·6H$_2$O**. The black and red lines represent the diffraction patterns at room temperature and 373 K, respectively.

considered to be driven by a structural transformation caused by the release of the water molecules. The emission maxima and vibronic structures of **MgPt-4** and **CaPt-4** are comparable and similar to those of **BaPt-4·5H$_2$O** and **SrPt-4·3H$_2$O**, implying that the structures of anhydrous **MgPt-4** and **CaPt-4** may be similar to that of **BaPt-4·5H$_2$O**, which has a 3-D coordination-bonded network structure. This structural transformation would affect the rigidity of the crystal lattice, leading to a change in the vibronic structures of their luminescence spectra.

Vapochromic and mechanochromic luminescence of MgPt·9H$_2$O.

In this section, we discuss the multichromic luminescence of **MgPt-4·9H$_2$O** in detail because it is the only complex that exhibits vapochromic and mechanochromic behaviours. Figure 7

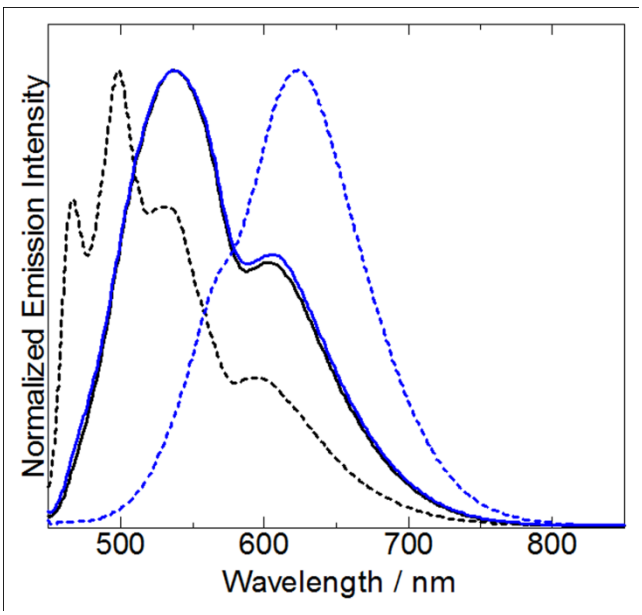

Fig. 7 Luminescence spectral changes in **MgPt-4·9H$_2$O** by mechanical grinding and exposure to MeOH vapour ($\lambda_{ex.}$ = 400 nm). The black and blue lines represent the spectra of as-synthesized and crushed crystals, respectively, whereas the dotted and solid lines represent the spectra before and after exposure to MeOH vapour for 1 day at room temperature, respectively.

shows the luminescence spectral changes in **MgPt-4·9H$_2$O** after grinding for 10 min and after exposing the samples to MeOH vapour for 1 day. The luminescence spectrum of the as-synthesized crystals changed from a greenish yellow $^3\pi$-π^* emission to a yellow emission centered at 537 nm with a shoulder at 607 nm after exposure to the MeOH vapour. The colour and emission were also changed to a reddish orange emission centered at 624 nm after mechanical grinding of the crystals, as shown in Figures 7 and 8. Interestingly, after exposing the crushed sample to MeOH vapour, it had almost the same yellow emission, with a maximum at 537 nm, as the as-synthesized crystals that had been exposed to MeOH vapour. The original emission of **MgPt-4·9H$_2$O** was gradually recovered by immersing these samples in water, even though **MgPt-4·9H$_2$O** is nearly insoluble in water. As summarized in Scheme 1, these results indicate that **MgPt-4·9H$_2$O** is a multichromic (vapo-, mechano-, and thermochromic) luminescent complex.

To investigate the mechanism of the vapochromic and mechanochromic behaviours, we measured PXRD patterns under various conditions. Figure 9 shows the changes in the PXRD pattern of **MgPt-4·9H$_2$O** upon mechanical grinding and exposure to MeOH vapour. Both the as-synthesized and crushed crystals showed almost the same diffraction patterns, suggesting that the

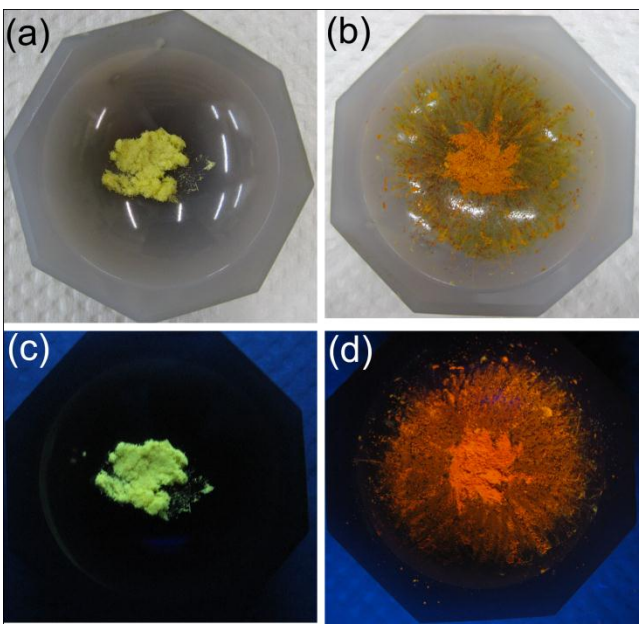

Fig. 8 Mechanochromic behaviour of **MgPt-4·9H$_2$O**. The upper and lower images are bright-field and luminescence images of (a, c) as-synthesized and (b, d) crushed crystals of **MgPt-4·9H$_2$O**, respectively.

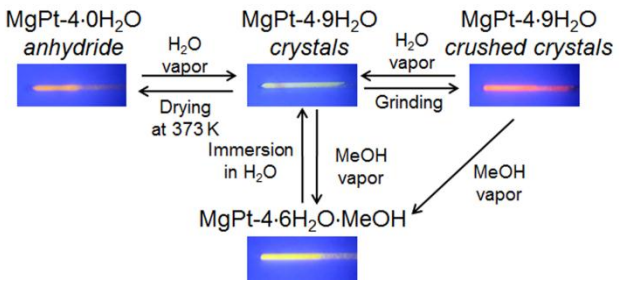

Scheme 1 Schematic diagram summarizing the multichromic behaviour of **MgPt-4·9H$_2$O**.

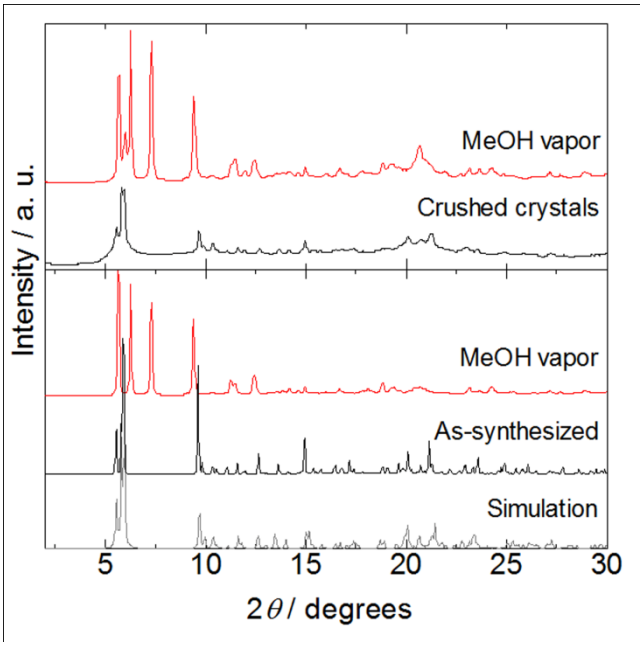

Fig. 9 Changes in the PXRD patterns of as-synthesized and crushed crystals of **MgPt-4·9H$_2$O** upon exposure to MeOH vapour for 2 days at room temperature (λ = 1.200(1) Å). The bottom gray pattern shows the simulation calculated from the crystal structure of **MgPt-4·9H$_2$O**.

long-range structure of **MgPt-4·9H$_2$O** was retained after mechanical grinding. It may be noted that the peak intensities and widths in the crushed sample were weaker and broader than those of the as-synthesized crystals in spite of the fact that both originated from the same amount of sample, which implies that the crystalline **MgPt-4·9H$_2$O** was partly transformed to an amorphous solid by mechanical grinding. A remarkable change was observed in the IR spectrum of the crushed **MgPt-4·9H$_2$O**. As shown in Figure 10(a), the overall spectral features of the as-synthesized and crushed crystals were quite similar. However, the ν(C≡N) mode of the cyano ligand was observed as two bands in the as-synthesized crystals, whereas it was observed as two bands with a shoulder at 2138 cm^{-1} in the crushed sample, which was not observed for any of the other crushed **MPt-4·*n*H$_2$O** crystals (see Figure S3). In addition, the elemental analysis of the crushed sample revealed that its chemical composition is the same as that of the as-synthesized **MgPt-4·9H$_2$O** (see supporting information). Thus, these results suggest that the observed mechanochromic behaviour of **MgPt-4·9H$_2$O** originates from the local structural change around the cyano ligand which might enhance the intermolecular metallophilic and/or π-π stacking interactions between the adjacent Pt(II) metalloligands. The PXRD pattern of as-synthesized **MgPt-4·9H$_2$O** also significantly changed upon its exposure to MeOH vapour. As shown in Figure 9, new intense diffraction peaks appeared at 6.2°, 7.3°, and 9.4°. A similar diffraction pattern was observed for the sample obtained from the exposure of crushed **MgPt-4·9H$_2$O** to MeOH vapour, suggesting that the structures of as-synthesized and crushed **MgPt-4·9H$_2$O** were the same after exposure to MeOH vapour. In the IR spectrum of **MgPt-4·9H$_2$O** that was exposed to MeOH vapour, the broad band assigned to the ν(O-H) mode of water molecules, appearing at 3400 cm^{-1}, seems to shift to a lower wavenumber as shown in Figure 10(b). New bands, assignable to the C-H, and C-

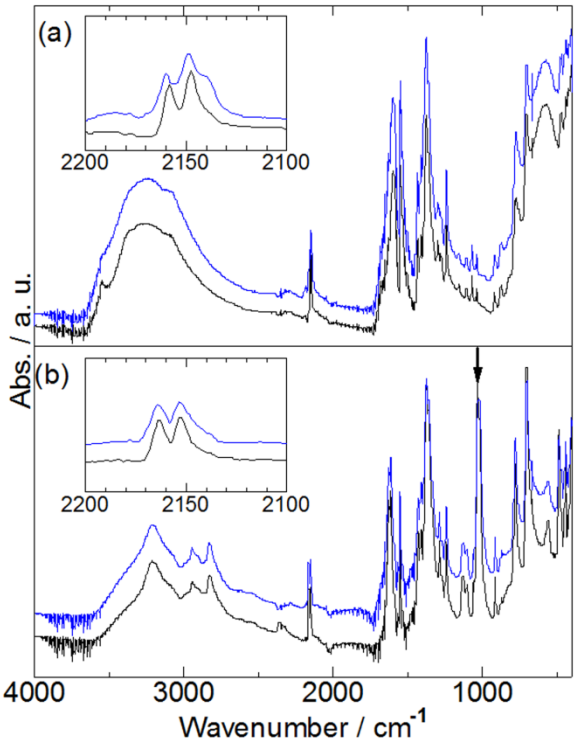

Fig. 10 IR spectra of as-synthesized (black) and crushed powder (blue) **MgPt-4·9H$_2$O** after exposure to (a) air and (b) MeOH vapour for 1 day. Insets show the expansion of the ν(C≡N) vibration band region around 2150 cm^{-1}. The black arrow shown in (b) indicates the ν(C-O) band of the adsorbed MeOH.

O stretching mode of the adsorbed MeOH molecule, were observed at 2944, 2829 and 1033 cm^{-1}, respectively, which are comparable to that of normal liquid MeOH. Similarly, under exposure the as-synthesized **MgPt-4·9H$_2$O** to methanol-d$_4$ vapour at room temperature, the bands assigned to ν(O-D), ν(C-D) and ν(C-O) bands of methanol-d$_4$ were appeared at around 2493, 2074 and 985 cm^{-1} and gradually increased, those energies are quite comparable to the normal liquid of methanol-d$_4$ (see Figure S4). These results suggest that the adsorbed MeOH molecule was not directly bonded to the Mg(II) ion. In the case of the crushed sample, the characteristic ν(C≡N) band at 2138 cm^{-1} disappeared after exposure to MeOH vapour. In addition, elemental analysis of the sample obtained after the exposure of **MgPt-4·9H$_2$O** to MeOH vapour for 1 day also suggests that three of the nine water molecules were replaced by one MeOH molecule to form **MgPt-4·6H$_2$O·MeOH** (see supporting information). In the TG-DTA analysis of the sample exposed to MeOH vapour, the gradual weight loss about 20.0% (at 400 K) was observed, which corresponds to the removal of all solvated water and methanol molecules in **MgPt-4·6H$_2$O·MeOH**. In addition, three endothermic peaks at 308, 325, and 335 K were observed for the methanol exposed sample, whereas the original **MgPt-4·9H$_2$O** showed only one endothermic peak at 321 K (see Figure S5). Thus, the vapochromic behaviour of **MgPt-4·9H$_2$O** is thought to originate from the exchange of water with MeOH, which induces a molecular rearrangement of the solid state. As mentioned above, four of the nine water molecules were not

bonded to the Mg(II) ion and formed 1-D water channels along the *a* axis, which may enable their easy exchange with MeOH. Although we have not yet succeeded in the structural determination of **MgPt-4·6H$_2$O·MeOH**, its emission energy and spectral shape suggest that the molecular rearrangement induced by guest exchange may enhance the intermolecular metallophilic and/or π-π stacking interaction, leading to a red shift of the emission band.

Effect of the position of carboxyl group in the metalloligand.

As mentioned in Introduction, we have previously reported the structures and chromic behaviours of the luminescent coordination polymers, **MPt-5**·*n*H$_2$O built from divalent M^{2+} ions (M = Zn^{2+}, Mg^{2+}, Ca^{2+}, Sr^{2+}, and Ba^{2+}) and the isomeric metalloligand $[Pt(CN)_2(5,5'\text{-dcbpy})]^{2-}$.[8] In this section, we discuss the effect of the position of carboxyl group on the metalloligand based on the comparison between **MPt-5** and **MPt-4** systems.

In the structures of **MPt-5**·*n*H$_2$O, one-dimensional coordination-bonded chain structure constructed by the alternate arrangement of M^{2+} ion and the metalloligand $[Pt(CN)_2(5,5'\text{-dcbpy})]^{2-}$ are commonly formed and the metallophilic interaction between Pt(II) ions is effective in all **MPt-5**·nH$_2$O complexes (scheme 2(a)). The bridging M^{2+} ions are bound by two carboxylate groups of the metalloligand at the axial position and several water molecules in the equatorial plane. The hydration numbers (n = 4 ~ 5) of **MPt-5** complexes are almost independent of the M^{2+} ion. By contrast, the crystal structures of **MPt-4** complexes strongly depend on the M^{2+} ion (scheme 2(b)). Except for the **MgPt-4**·9H$_2$O, the bridging M^{2+} ions are surrounded by two or three carboxylate groups of the metalloligand, and the hydration numbers of **MPt-4** complexes strongly depend on the M^{2+} ion and are in the range from 3 to 9. It should be emphasized that the intermolecular metallophilic interaction in the **MPt-5** system is thought to be effective in the uniformly stacked Pt(II)-complex columns, whereas it is only effective in the dimerized structure in all the fully-hydrated **MPt-4**·*n*H$_2$O complexes except for the **MgPt-4**·9H$_2$O in which there is no metallophilic interaction. In addition, the sodium salt of the metalloligand, Na$_2$[Pt(CN)$_2$(4,4'-dcbpy)]·5H$_2$O has also no metallophilic interaction.[6p] Consequently, emission properties of **MPt-5** and **MPt-4** systems are quite different to each other, i.e., the **MPt-5** complexes exhibit the red emission derived from the ^{3}MMLCT state with relatively short emission lifetime ($\tau_{em.}$ = 25 - 69 ns) with small quantum yields (Φ_{em} = 0.05 - 0.12), whereas the **MPt-4** complexes shows the green to yellow emission originating from the ^{3}π-π* excited state with long emission lifetime ($\tau_{em.}$ = 0.27 - 3.27 μs) and large quantum yields (Φ_{em} = 0.09 - 0.27). In addition, the **MPt-5** complexes commonly exhibit interesting solid-state solvatochromic behaviour driven by the adsorption/desorption of the hydration water molecules, whereas the chromic behaviours of **MPt-4** complexes strongly depend on the M^{2+} ion as discussed above. These differences clearly indicate that the position of the carboxyl group attached on the bipyridine ligand plays an important role on these **MPt** systems. Considering the fact that the acid-dissociation constants of 4,4′-H$_2$dcbpy and 5,5′-H$_2$dcbpy are very close to each other,[17] the positional difference of the coordination-bonding site gives considerable effects on the coordination-network structures including the intermolecular metallophilic interaction. In addition, more negative reduction potential of the 4,4′-dcbpy ligand than that of 5,5′-dcbpy[17] may affect the emission properties of these Pt(II)-diimine-based complex salts.

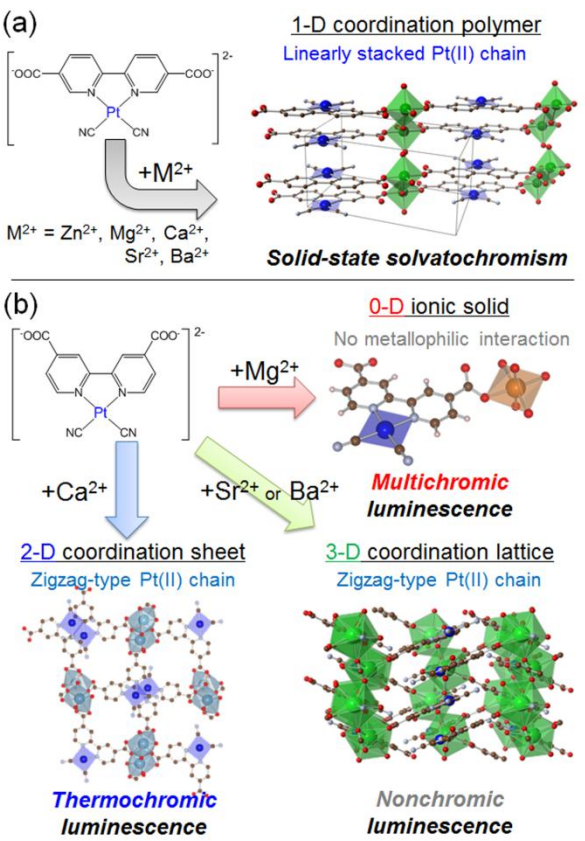

Scheme 2 Schematic diagram summarizing the differences of structures and luminescence properties between (a) **MPt-5** and (b) **MPt-4** systems.

Conclusion

We synthesized four new Pt(II)-diimine-based complex salts with alkaline-earth metal ions, namely, {[Mg(H$_2$O)$_5$][Pt(CN)$_2$(4,4'-dcbpy)]·4H$_2$O} (**MgPt-4·9H$_2$O**), {[Ca(H$_2$O)$_3$][Pt(CN)$_2$(4,4'-dcbpy)]·3H$_2$O} (**CaPt-4·6H$_2$O**), {[Sr(H$_2$O)$_2$][Pt(CN)$_2$(4,4'-dcbpy)]·H$_2$O} (**SrPt-4·3H$_2$O**), and {[Ba(H$_2$O)$_2$][Pt(CN)$_2$(4,4'-dcbpy)]·3H$_2$O} (**BaPt-4·5H$_2$O**). Single-crystal X-ray structural determination revealed that there were water channels in their crystals and that the metallophilic interaction between Pt(II) ions was negligibly weak in **MgPt-4·9H$_2$O** and moderate in the other three **MPt-4·nH$_2$O**, which formed dimerized structures. There was no coordination network in the **MgPt-4·9H$_2$O**, but two- and three-dimensional rigid coordination networks were formed in **CaPt-4·6H$_2$O** and the other two complexes, respectively. These structures are quite different to the Pt(II)-diimine-based **MPt-5** system with the isomeric metalloligand, $[Pt(CN)_2(5,5'\text{-dcbpy})]^{2-}$.[8] All of the complexes exhibited ^{3}π-π* emission with similar vibronic structures. **MgPt-4·9H$_2$O** was found to be triple-chromic (thermo-, mechano-, and vapochromic) luminescent materials. **CaPt-4·6H$_2$O** showed only the thermochromic luminescence and the other two complexes that featured heavier alkaline-earth metal ions did not exhibit any chromic behaviour. The thermochromic luminescence of the former two complexes is

mainly derived from the adsorption/desorption of water. The large amount of water molecules included in **MgPt-4·9H$_2$O** may enable it to respond to guest exchange and mechanical grinding, leading to the interesting multichromic luminescence. Further study on the fine tuning of the structural flexibility to control the multichromic behaviour is now in progress.

Acknowledgements

We thank Prof. S. Noro (Hokkaido Univ.) for his kind experimental support and helpful discussion. This work is supported by a Grant-in-Aid for Scientific Research (B)(23350025), Photochromism (No.471), Coordination Programming (No. 2107), Young Scientists (B) (19750050), and the Global COE Program (Project No. B01: Catalysis as the Basis for Innovation in Materials Science) from MEXT, Japan.

Notes and references

[a] *Division of Chemistry, Faculty of Science, Hokkaido University, North-10 West-8, Kita-ku, Sapporo 060-0810, Japan. Fax: 81-11-706-3447; Tel:81-11-706-3817; E-mail: akoba@sci.hokudai.ac.jp (A.K.), mkato@sci.hokudai.ac.jp (M. K.)*

† Electronic Supplementary Information (ESI) available: X-ray crystallographic files in CIF format (CCDC reference numbers 829255, 829256, 848114 and 829257); TG curves of the **MPt-4·*n*H$_2$O** series; PXRD patterns of **BaPt-4·5H$_2$O** at 298 and 373 K; IR spectra of as-synthesized and crushed crystals of **CaPt-4·6H$_2$O**; IR spectral change of as-synthesized **MgPt-4·9H$_2$O** under exposure to methanol-d$_4$ vapour; TG-DTA curves of **MgPt-4·9H$_2$O** and **MgPt-4·6H$_2$O·MeOH**; bond lengths around the $[Pt(CN)_2(4,4'\text{-dcbpy})]^{2-}$ of **MgPt-4·9H$_2$O**, **CaPt-4·6H$_2$O**, and **BaPt-4·5H$_2$O**; elemental analyses for **MgPt-4·9H$_2$O** after grinding and exposure to MeOH vapour for 1 day. See DOI: 10.1039/b000000x/

1 (a) M. Hissler, J. E. McGarrah, W. B. Connick, D. K. Geiger, S. D. Cummings, R. Eisenberg, *Coord. Chem. Rev.* 2000, **208**, 115-137. (b) M. Kato, *Bull. Chem. Soc. Jpn.* 2007, **80**, 287-294. (c) K. M.-C. Wong, V. Y.-W. Yam, *Coord. Chem. Rev.* 2007, **251**, 2477-2488. (d) I. Eryazici, C. N. Moorefield, G. R. Newkome, *Chem. Rev.* 2008, **108**, 1834-1895. (e) J. A. GarethWilliams, S. Develay, D. L. Rochester, L. Murphy, *Coord. Chem. Rev.* 2008, **252**, 2596-2611. (f) R. McGuire Jr., M. C. McGuire, D. R. McMillin, *Coord. Chem. Rev.* 2010, **254**, 2574-2583.

2 (a) S. F. Rice, H. B. Gray, *J. Am. Chem. Soc.* 1983, **105**, 4571-4575. (b) S. D. Cummings, R. Eisenberg, *J. Am. Chem. Soc.* 1996, **118**, 1949-1960. (c) W. B. Connick, H. B. Gray, *J. Am. Chem. Soc.* 1997, **119**, 11620-11627. (d) V. W.-W. Yam. R. P.-L. Tang, K. M.-C. Wong, K.-K. Cheung, *Organometallics* 2001, **20**, 4476-4482. (e) S. Huertas, M. Hissler, J. E. McGarrah, R. L. Lachicotte, R. Eisenberg, *Inorg. Chem.* 2001, **40**, 1183-1188. (f) V. W.-W. Yam, K. M.-C. Wong, N. Zhu, *J. Am. Chem. Soc.* 2002, **124**, 6506-6507. (g) S.-W. Lai, H.-W. Lam, K.-K. Cheung, C.-M. Che, *Organometallics* 2002, **21**, 226-234. (h) V. W.-W. Yam, K. H.-Y. Chan, K. M.-C. Wong, N. Zhu, *Chem. Eur. J.* 2005, **11**, 4535-4543. (i) M. Kato, Y. Shishido, Y. Ishida, S. Kishi, *Chem. Lett.* 2008, **37**, 16-17.

3 (a) C.-M. Che, L.-Y. He, C.-K. Poon, T. C. W. Mak, *Inorg. Chem.* 1989, **28**, 3081-3083. (b) V. M. Miskowski, V. H. Houlding, *Inorg. Chem.* 1991, **30**, 4446-4452. (c) J. A. Bailey, M. G. Hill, R. E. Marsh, V. M. Miskowski, W. P. Schaefer, H. B. Gray, *Inorg. Chem.* 1995, **34**, 4591-4599. (d) W. B. Connick, L. M. Henling, R. E. Marsh, H. B. Gray, *Inorg. Chem.* 1996, **35**, 6261-6265. (e) M. Kato, C. Kosuge, K. Morii, J. S. Ahn, H. Kitagawa, T. Mitani, M. Matsushita, T. Kato, S. Yano, M. Kimura, *Inorg. Chem.* 1999, **38**, 1638-1641. (f) M. Kato, S. Kishi, *Inorg. Chem.* 2003, **42**, 8728-8734.

4 (a) T. Koshiyama, A. Omura, M. Kato, M. *Chem. Lett.* 2004, **33**, 1386-1387. (b) B. Ma, J. Li, P. I. Djurovich, M. Yousufuddin, R. Bau, M. E. Thompson, *J. Am. Chem. Soc.* 2005, **127**, 28-29. (c) A. A. Rachford, F. N. Castellano, *Inorg. Chem.* 2009, **48**, 10865-10867. (d) R. Aoki, A. Kobayashi, H.-C. Chang, M. Kato, *Bull. Chem. Soc. Jpn.* 2011, **84**, 218-225.

5 (a) C. L. Exstrom, J. E. Sowa Jr., C. A. Daws, D. Janzen, K. R. Mann, G. A. Moore, F. F. Stewart, *Chem. Mater.* 1995, **7**, 15-17. (b) C. A. Daws, C. L. Exstrom, J. R. Sowa Jr., K. R. Mann, *Chem. Mater.* 1997, **9**, 363-368. (c) C. E. Buss, C. E. Anderson, M. K. Pomije, C. M. Lutz, D. Britton, K. R. Mann, *J. Am. Chem. Soc.* 1998, **120**, 7783-7790. (d) Y. Kunugi, K. R. Mann, L. L. Miller, C. L. Exstrom, *J. Am. Chem. Soc.* 1998, **120**, 589-590. (e) Y. Kunugi, L. L. Miller, K. R. Mann, M. K. Pomije, *Chem. Mater.* 1998, **10**, 1487- 1489.

6 (a) W. Lu, M. C. W. Chan, K.-K. Cheung, C.-M. Che, *Organometallics* 2001, **20**, 2477-2486. (b) S. M. Drew, D. E. Janzen, C. E. Buss, D. I. MacEwan, K. M. Dublin K. R. Mann, *J. Am. Chem. Soc.*, 2001, **123**, 8414-8415. (c) C. E. Buss, K. R. Mann, *J. Am. Chem. Soc.* 2002, **124**, 1031-1039. (d) M. Kato, A. Omura, A. Toshikawa, S. Kishi, Y. Sugimoto, *Angew. Chem.* 2002, **114**, 3315-3317; *Angew. Chem. Int. Ed.* 2002, **41**, 3183-3185. (e) S. Kishi, M. Kato, *Mol. Cryst. Liq. Cryst.*, 2002, **379**, 303-308. (f) W. Lu, M. C. W. Chan, N. Zhu, C.-M. Che, Z. He, K.-Y. Wong, *Chem. Eur. J.* 2003, **9**, 6155-6166. (g) L. J. Grove, J. M. Rennekamp, H. Jude, W. B. Connick, *J. Am. Chem. Soc.* 2004, **126**, 1594-1595. (h) M. Kato, S. Kishi, Y. Wakamatsu, Y. Sugi, Y. Osamura, T. Koshiyama, M. Hasegawa, *Chem. Lett.* 2005, **34**, 1368-1369. (i) S. C. F. Kui, S. S.-Y. Chui, C.-M. Che, N. Zhu, *J. Am. Chem. Soc.* 2006, **128**, 8297-8309. (j) P. Du, J. Schneider, W. W. Brennessel, R. Eisenberg, *Inorg. Chem.* 2008, **47**, 69-77. (k) L. J. Grove, A. G. Oliver, J. A. Krause, W. B. Connick, *Inorg. Chem.* 2008, **47**, 1408-1410. (l) J. Fornies, S. Fuertes, J. A. Lopez, A. Martin, V. Sicilia, *Inorg. Chem.* 2008, **47**, 7166-7176. (m) M. L. Muro, C. A. Daws, F. N. Castellano, *Chem. Commun.* 2008, 6134-6136. (n) A. Kobayashi, Y. Fukuzawa, S. Noro, T. Nakamura, M. Kato, *Chem. Lett.* 2009, **38**, 998-999. (o) J. Ni, Y.-H. Wu, X. Zhang, B. Li, L.-Y. Zhang, Z.-N. Chen, *Inorg. Chem.* 2009, **48**, 10202-10210. (p) A. Kobayashi, T. Yonemura, M. Kato, *Eur. J. Inorg. Chem.* 2010, 2465–2470. (r) J. S. Field, C. D. Grimmer, O. Q. Munro, B. P. Waldron, *Dalton Trans.* 2010, **39**, 1558-1567. (s) Á Díez, J. Forniés, C. Larraz, E. Lalinde, J. A. López, A. Martín, M. T. Moreno, V. Sicilia, *Inorg. Chem.* 2010, **49**, 3239-3251. (t) Y. Nishiuchi, A. Takayama, T. Suzuki, K. Shinozaki, *Eur. J. Inorg. Chem.* 2011, **11**, 1815-1823. (u) Z. M. Hudson, C. Sun, K. J. Harris, B. E. G. Lucier, R. W. Schurko, S. Wang, *Inorg. Chem.* 2011, **50**, 3447-3457.

7 (a) H. Ito, T. Saito, N. Oshima, N. Kitamura, S. Ishizaka, Y. Hinatsu, M. Wakeshima, M. Kato, K. Tsuge, M. Sawamura, *J. Am. Chem. Soc.* 2008, **130**, 10044-10045. (b) T. Abe, T. Itakura, N. Ikeda, K. Shinozaki, *Dalton Trans.* 2009, 711-715. (c) A. Laguna, T. Lasanta, J. M. López-de-Luzuriaga, M. Monge, P. Naumov, M. E. Olmos, *J. Am. Chem. Soc.* 2010, **132**, 456-457. (d) J. Ni, X. Zhang, Y.-H. Wu, L.-Y. Zhang, Z.-N. Chen, *Chem. Eur. J.* 2011, **17**, 1171-1183.

8 (a) A. Kobayashi, H. Hara, S. Noro, M. Kato, *Dalton Trans.* 2010, **39**, 3400-3406. (b) H. Hara, A. Kobayashi, S. Noro, H.-C. Chang, M. Kato, *Dalton Trans.* 2011, **40**, 8012-8018.

9 (a) H. Li, M. Eddaoudi, M. O'Keeffe, O. M. Yaghi, *Nature* 1999, **402**, 276-279. (b) M. Eddaoudi, D. B. Moler, H. Li, B. Chen, T. M. Reineke, M. O'Keeffe, O. M. Yaghi, *Acc. Chem. Res.* 2001, **34**, 319-330. (c) N. L. Rosi, J. Kim. M. Eddaoudi, B. Chen, M. O'Keeffe, O. M. Yaghi, *J. Am. Chem. Soc.* 2005, **127**, 1504-1518. (d) T. Louseau, G. Férey, *J. Fluor. Chem.* 2007, **128**, 413-422. (e) R. Banerjee, A. Phan. B. Wang, C. Knobler, H. Furukawa, M. O'Keeffe, O. M. Yaghi, *Science* 2008, **319**, 939-943. (f) G. Férey, C. Serre, *Chem. Soc. Rev.* 2009, **38**, 1380-1399. (g) D. J. Tranchemontagne, J. L. Mendoza-Cortes, M. O'Keeffe, O. M. Yaghi, *Chem. Soc. Rev.* 2009, **38**, 1257-1283.

10 (a) G. J. Halder, C. J. Kepert, B. Moubaraki, K. S. Murray, J. D. Cashion, *Science* 2002, **298**, 1762-1765. (b) S. Kitagawa, R. Kitaura, S. Noro, *Angew. Chem. Int. Ed.* 2004, **43**, 2334-2375. (c) R. Matsuda, R. Kitaura, S. Kitagawa, Y. Kubota, R. V. Belosludov, T. C. Kobayashi, H. Sakamoto, T. Chiba, M. Takata, Y. Kawazoe, Y. Mita, *Nature* 2005, **436**, 238-241. (d) O. M. Yaghi, *Nat. Mater.* 2007, **6**, 92-93. (e) B. D. Chandler, G. D. Enright, K. A. Udachin, S. Pawsey, J. A. Ripmeester, D. T. Cramb, G. K. H. Shimizu, *Nat. Mater.* 2008, **7**, 229-235. (f) D. Tanaka, K. Nakagawa, M. Higuchi, S. Horike, Y.

Kubota, T. C. Kobayashi, M. Takata, S. Kitagawa, *Angew. Chem. Int. Ed.* 2008, **47**, 3914-3918. (g) J.-R. Li, R. J. Kuppler, H.-C. Zhou, *Chem. Soc. Rev.* 2009, **38**, 1477-1504. (h) S. Horike, S. Shimomura, S. Kitagawa, *Nat. Chem.* 2009, **1**, 695-704. (f) M. Higuchi, D. Tanaka, S. Horike, H. Sakamoto, K. Nakamura, Y. Takashima, Y. Hijikata, N. Yanai, J. Kim, K. Kato, Y. Kubota, M. Takata, S. Kitagawa, *J. Am. Chem. Soc.* 2009, **131**, 10336-10337. (i) T. Fukushima, S. Horike, Y. Inabushi, K. Nakagawa, Y. Kubota, M. Takata, S. Kitagawa, *Angew. Chem. Int. Ed.* 2010, **49**, 4820-4824.

11 (a) D.-Y. Hong, Y. K. Hwang, C. Serre, G. Férey, J.-S. Chang, *Adv. Funct. Mater.* 2009, **19**, 1537-1552. (b) A. M. Shultz, O. K. Farha, J. T. Hupp, S. T. Nguyen, *J. Am. Chem. Soc.* 2009, **131**, 4204-4205. (c) L. Yang, S. Kinoshita, T. Yamada, S. Kanda, H. Kitagawa, M. Tokunaga, T. Ishimoto, T. Ogura, R. Nagumo, A. Miyamoto, M. Koyama, *Angew. Chem. Int. Ed.* 2010, **49**, 5348-5351. (d) A. Dhakshinamoorthy, M. Alvaro, H. Garcia, *Chem. Commun.* 2010, **46**, 6476-6478.

12 *CrystalClear*, Molecular Structure Corporation, Orem, UT, 2001.

13 *SIR2004*, M. C. Burla, R. Caliandro, M. Camalli, B. Carrozzini, G. L. Cascarano, L. De Caro, C. Giacovazzo, G. Polidori, R. Spagana, *J. Appl. Cryst.* 2005, **38**, 381-388.

14 *SHLEX97*, G. M. Sheldrick, *Acta Crystallogr. Sect. A*, 2008, **64**, 112-122.

15 A. L. Spek, *J. Appl. Cryst.* 2003, **36**, 7-13.

16 *CrystalStructure 3.8*, Crystal Structure Analysis Package, Rigaku and Rigaku/MSC (2000-2006), 9009 New Trails Dr , The Woodlands TX 77381 USA.

17 Md. K. Nazeeruddin, K. Kalyanasundaram, *Inorg. Chem.* 1989, **28**, 4251-4259.

18 These pictures were drawn by VESTA computer program. K. Momma, F. Izumi, *J. Appl. Crystallogr.* 2008, **41**, 653-658.